Supporting Information for

Tumor Acidity/NIR Controlled Interaction of Transformable Nanoparticle with Biological Systems for Cancer Therapy

Dongdong Li,[†,‡] Yinchu Ma,[‡] Jinzhi Du,[†] Wei Tao,[‡] Xiaojiao Du,[†] Xianzhu Yang,[†,‡] and Jun Wang*[†]*

[†] Institutes for Life Sciences, School of Medicine and National Engineering Research Center for Tissue Restoration and Reconstruction, South China University of Technology, Guangzhou, Guandong 510006, P. R. China

[‡] School of Medical Engineering, Hefei University of Technology, Hefei, Anhui 230009, P. R. China

[§] These authors contributed equally.

* Address correspondence to: yangxz@hfut.edu.cn (X. Yang), and jwang699@ustc.edu.cn (J. Wang)

MATERIALS AND METHODS

Materials. Maleimide-terminated PEG-*b*-PHEP (Mal-PEG_{77}-*b*-$PHEP_{25}$, the subscript number represents the degrees of polymerization of each block) was synthesized by ring-opening polymerization of cyclic phosphoester monomer 2-hexoxy-2-oxo-1,3,2-dioxaphospholane (HEP) using Maleimide-terminated PEG (Mn = 3350, Sigma-Aldrich, USA) as the initiator, and the degrees of polymerization was calculated according its ^1H NMR (Figure S1). The TAT (YGRKKRRQRRRC-NH_2) was purchased from Chinese Peptide Company (Hangzhou, China). Doxorubicin hydrochloride (DOX•HCl) was prepared from Hisun Pharmaceutical Co. Ltd. (Zhejiang, China). 3-(4,5-Dimethylthiazol-2-yl)-2,5-diphenyl tetrazolium bromide (MTT), Alexa Fluor® 488 phalloidin, 4',6-diamidino-2-phenylindol) (DAPI), ethylenediaminetetraacetic acid (EDTA), 5,5'-Dithiobis(2-nitrobenzoic acid) (DTNB, Ellman's reagent), and IR-780 iodide were purchased from Sigma-Aldrich (St. Louis, MO, USA). Fetal bovine serum (FBS) and Dulbecco's Modified Eagle Medium (DMEM) were purchased from Gibco BRL (Eggenstein, Germany) and Hyclone (Zhejiang, China), respectively. Other organic solvents or reagents were of analytic grade and used as received.

Characterizations. Nuclear magnetic resonance (NMR) spectra were recorded in deuterated reagent (such as, $CDCl_3$ or DMSO-d_6) with an Agilent VNMRS 600 MHz NMR spectrometer (California, USA). The size and size distribution of nanoparticle in aqueous solution were measured by DLS carried out on a Brookhaven NanoBrook-90 Plus (Brookhaven Instrument Corporation, New York, USA) apparatus with a solid laser (35 mW, 640 nm) and 90° collecting optics. The concentration of doxorubicin (DOX) and IR-780

iodide was determined by Fluorescence spectrometer (HITACHI F-2700, Tokyo, Japan) and Ultraviolet spectrophotometer (HITACHI U-5100, Tokyo, Japan). The morphology of the nanoparticle was examined by JEM-2100F transmission electron microscopy (TEM) at an accelerating voltage of 200 kV. The absorption spectra were measured on a measured on a UV-3802 (UNICO, China) spectrophotometer.

Synthesis of TAT-PEG-*b*-PHEP. Mal-PEG_{77}-*b*-$PHEP_{25}$ (100.0 mg, 0.012 mmol) was dissolved in 10.0 mL of DMSO. The ultrapure water (100.0 mL) was poured into the DMSO solution under gentle stirring. After stirring for an additional 3 h, the solution was loaded into a dialysis bag (MWCO 14000 Da) and against with ultrapurified water overnight. The TAT peptide (20.0, 0.012 mmol), which was chemically conjugated to Mal-PEG_{77}-*b*-$PHEP_{25}$ through a covalent thiol-maleimide linkage, was added into the obtained micelles under N_2 atmosphere at equal molar ratio. After stirring at the room temperature for 24 h, the reaction solution was centrifuged at 30,000 g for 1 h to collect the sample; the supernatant was obtained, and the cysteine residues' thiol group of TAT was reacted with Ellman's reagent DTNB (78 μg/mL in 0.1 M sodium phosphate buffer, pH 8.0, containing 1mM EDTA) at room temperature for 15 min, followed by absorbance measurement at 412 nm. The concentration of unreacted free TAT peptide in the supernatant was determined using the calibration curve prepared from TAT peptide standards. Then, conjugation efficacy (83.5%) was determined by subtracting the amount of free TAT peptide in the total TAT peptide.

Preparation of IR-780- and DOX-loaded nanoparticle. The IR-780- and DOX-loaded nanoparticle TAT-$NP_{IR\&DOX}$ was prepared by a dialysis method. Briefly, a mixture containing 10.0 mg of TAT-PEG-*b*-PHEP, 1.0 mg of DOX and 1.0 mg of IR-780 was dissolved in 1.5

mL DMSO solution. After stirring for 30 min, the phosphate buffer saline (PBS, pH 7.4, 0.01 M) was poured into and continuously stirred for 4 h. The mixture were loaded into a dialysis bag (MWCO 14000 Da) and dialyzed against with 2 L pH 7.4 PBS (0.01 M) overnight. The solution was filtered through a 0.45 μm filter to remove the unloaded DOX and IR-780.

Furthermore, the TAT peptides of TAT-$NP_{IR\&DOX}$ was modified with the 2,3-dimethylmaleic anhydride (DA). The reaction was performed as follows: 5 equivalents (to TAT lysine residues' amines) of DA were gradually added into TAT-$NP_{IR\&DOX}$ solution. The pH of solution was kept in the range of 8-9 by addition of NaOH solution (1 M). The reaction was continued at room temperature for 4 h. After ultrafiltration using Amicon YM-30 centrifugal filter devices (Millipore, MWCO 3000 Da), the obtained nanoparticles was obtained and denoted as ^{DA}TAT-$NP_{IR\&DOX}$. The ^{SA}TAT-$NP_{IR\&DOX}$ was synthesized similarly by replacing DA with succinic anhydride (SA). According to the UPLC analysis, the loading content of IR-780 and DOX for TAT-$NP_{IR\&DOX}$, ^{DA}TAT-$NP_{IR\&DOX}$, and ^{SA}TAT-$NP_{IR\&DOX}$ was ca. 2.18±0.23% and 4.36±0.17%, respectively.

As a control, the DOX and IR-780 were separately encapsulated into ^{DA}TAT-PEG-*b*-PHEP based nanoparticle, which was denoted as ^{DA}TAT-NP_{IR}/^{DA}TAT-NP_{DOX}. Additionally, the blank nanoparticle TAT-NP, ^{DA}TAT-NP, or ^{SA}TAT-NP were also prepared by the similar methods when the DOX and IR-780 was absent.

The tumor acidity-activated TAT Peptide by ^{1}H NMR spectroscopy. The blank nanoparticle ^{DA}TAT-NP and ^{SA}TAT-NP was dispersed in PBS buffer (pH 6.5, 0.01 M) in 37 °C water bath with shaking. After incubation for 30 min, the solution was collected and

freeze dried. The lyophilized samples were dissolved in DMSO-d_6 and characterized by a 600 MHz ^{1}H NMR spectrometer.

Changes of zeta potential of these nanoparticles at different pH. The nanoparticle TAT-NP$_{IR\&DOX}$, ^{DA}TAT-NP$_{IR\&DOX}$, and ^{SA}TAT-NP$_{IR\&DOX}$ were dispersed in pH 7.4 and 6.5 PBS (0.01 M) at the concentration of 1.0 mg/mL and incubated at 37 °C. Then, the samples were taken at designated time point and the zeta potentials were measured by Brookhaven NanoBrook-90 Plus Zeta.

Degradation of the amide bonds formed between TAT lysine residues' amines and DA or SA: ^{DA}TAT-NP and ^{SA}TAT-NP was dispersed in PB buffer (0.02 M) at pH 6.5 and 7.4 for preset times. Then fluorescamine in DMF (2 mg/mL, 0.2 mL, Shanghai macklin biochemical Co. Ltd., China) was added to samples (1.0 mL).[1] After further incubation for 10 min at 37 °C, the fluorescence intensity (Fs) was tested *via* a fluorescence spectrophotometer (Ex: 390 nm, Em: 483 nm). Fo was defined as the fluorescence of TAT-NP with same concentration, which contained the equivalent primary amine group to that all the amide bonds of ^{DA}TAT-NP or ^{SA}TAT-NP was hydrolyzed, while Fc was defined as the fluorescence of PBS control. The degradation rate of DA was calculated as following: (Fs−Fc)/(Fo−Fc) × 100%. The degradation of SA in ^{SA}TAT-NP/Pt at pH 7.4 or 6.8 was also investigated with the same method.

Photothermal effects of nanoparticle. The TAT-NP$_{IR\&DOX}$, ^{DA}TAT-NP$_{IR\&DOX}$, ^{SA}TAT-NP$_{IR\&DOX}$ and ^{DA}TAT-NP$_{IR}$/^{DA}TAT-NP$_{DOX}$ (200 μL) with IR-780 concentration at 2.0 μg/mL was irradiated under a 808 nm laser sources (New Industries Optoelectronics, Changchun, China) at a power density of 1.0 W/cm^2 for 5 min. The ultrapure water was used

as a negative control. The change of real-time temperature was detected by an infrared camera (ICI7320, Infrared Camera Inc., Texas, USA) and analyzed using IR Flash thermal imaging analysis software.

In vitro **drug release.** ^{DA}TAT-NP$_{IR\&DOX}$, ^{SA}TAT-NP$_{IR\&DOX}$, TAT-NP$_{IR\&DOX}$, and ^{DA}TAT-NP$_{IR}$/^{DA}TAT-NP$_{DOX}$ ([IR-780] = 2.0 μg/mL, [DOX] = 4.0 μg/mL) were exposed to 808 nm laser at a power density of 1.0 W/cm^2. After 5 min irradiation, the samples (1.0 mL) were transferred into the dialysis bag (MWCO 3500 Da) and suspended in 20 mL PBS buffer (0.01 M, pH 7.4 or 6.5) at 37 °C with mild shaking. Collected external PBS buffer at different periods, the external PBS buffer was replaced with equal volume of fresh PBS buffer, The collected solution was freeze-dried and redissolved in the mixture solution of acetonitrile/water (50/50, v/v) to determine the concentration of doxorubicin by UPLC (Agilent 1290 Infinity II, California, USA). Moreover, ^{DA}TAT-NP$_{IR}$/^{DA}TAT-NP$_{DOX}$ was pre-incubated in 45 °C for 5 min, and then the DOX release was also determined.

Intraparticle temperature measurement using fluorescence lifetime. 250 μL of TAT-NP$_{IR\&DOX}$, ^{DA}TAT-NP$_{IR\&DOX}$, ^{SA}TAT-NP$_{IR\&DOX}$ and ^{DA}TAT-NP$_{IR}$/^{DA}TAT-NP$_{DOX}$ nanoparticle ([IR-780] = 2.0 μg/mL, [DOX] = 4.0 μg/mL) aqueous solution was first heated at various temperature, and then the DOX fluorescence lifetime of these formulations was measured using a FLS920 time-resolved and steady-state fluorescence spectrometer (Edinburgh Instruments, UK) with a 488 nm excitation source and the detector at 520 nm. The average excited state decay times (τ_{av}) were then obtained, and then the lifetime change was calculated according to the following formula: $\Delta\tau_{av} = \tau_{av}$(T °C)- τ_{av}(25.0 °C). A standard curve was obtained by plotting the lifetime change $\Delta\tau_{av}$ against temperature.

To determine the intraparticle temperature, 250 μL of TAT-$NP_{IR\&DOX}$, ^{DA}TAT-$NP_{IR\&DOX}$, ^{SA}TAT-$NP_{IR\&DOX}$ and ^{DA}TAT-NP_{IR}/^{DA}TAT-NP_{DOX} ([IR-780] = 2.0 μg/mL, [DOX] = 4.0 μg/mL) aqueous solution was were exposed to NIR irradiation (808 nm, 1.0 W/cm^2, 5.0 min), and then DOX fluorescence lifetime was detected as described above, and the intraparticle temperature was obtained according the above standard curve.

Cell culture. The human breast cancer cell line MDA-MB-231 and murine macrophage cell line RAW264.7 were obtained from the American Type Culture Collection (ATCC). The RAW264.7 and MDA-MB-231 cells were cultured in complete RPMI-1640 complete and DMEM medium (containing 10 % FBS) at 37 ^{o}C in a 5% CO_2 atmosphere.

Cell uptake by macrophage cells and tumor cells. RAW 264.7 cells were seeded into 24-well plates at 8.0 × 10^4 cells per well with 0.5 mL complete RPMI-1640 medium. After incubation at 37 °C with 5% CO_2 overnight, the original medium was replaced with TAT-$NP_{IR\&DOX}$, ^{DA}TAT-$NP_{IR\&DOX}$, ^{SA}TAT-$NP_{IR\&DOX}$, and IR&DOX (4.0 μg/mL of DOX and 2.0 μg/mL of IR-780). After further incubated for 2 h, the cells were washed twice with fresh PBS, trypsinized, and collected for FACS analyses (FACS Calibur flow cytometer, BD Biosciences, USA).

To examine the cellular uptake by tumor cells, MDA-MB-231 cells were seeded into 24-well plates at 1 × 10^5 cells per well with 0.5 mL complete DMEM medium. After incubation at 37 °C with 5% CO_2 overnight, the cells was replaced by these nanoparticles as described above at pH 6.5 and pH 7.4. After further incubated for 2 h, the cells were washed twice with fresh PBS, trypsinized, and collected for FACS analyses (FACS Calibur flow cytometer, BD Biosciences, USA) and UPLC analyses.

In addition, in order to analyze the cellular uptake of DOX, the MDB-MA-231 cells were seeded on coverslips in a 24-well plate. After 24 h of incubation, the cells treated as mentioned above, and then the cell membrane were stained by Alexa Fluor 488 (green), and cell nuclei were stained by DAPI (blue). The cellular uptake behavior was visualized under a confocal laser scanning microscope (CLSM).

Intracellular DOX release controlled by NIR irradiation. MDA-MB-231cells were seeded in 24-well plates at 5×10^4 cells per well with 0.5 mL complete DMEM medium. After incubation at 37 ^oC with 5% CO_2 overnight, the medium was replaced by fresh complete DMEM medium containing ^{DA}TAT-NP$_{IR\&DOX}$, and ^{DA}TAT-NP$_{IR}$/^{DA}TAT-NP$_{DOX}$ (4.0 μg/mL of DOX and 2.0 μg/mL of IR-780). After incubation 1 h, the cells were washed twice with fresh DMEM medium, irradiated under 808 nm NIR laser (1.0 W/cm^2 for 5 min). After further 4 h of incubation, the cells were washed with PBS, trypsinized, and collected for FACS analyses (FACS Calibur flow cytometer, BD Biosciences, USA). In additionally, for CLSM observation, the cells treated with the same procedure were stained with DAPI (blue) for cell nuclei, Lysotracke (green) for cell lysosome and were observed by CLSM (LSM 710, Carl Zeiss, Inc., Jena, Germany).

Animals and tumor model. Balb/c nude mice (6~8 weeks old) were purchased from the Beijing HFK Bioscience Co. Ltd.(Beijing, China) and all animals received care in compliance with the guidelines outlined in the Guide for the Care and Use of Laboratory Animals. The procedures were approved by the Hefei University of Technology Animal Care and Use Committee. Approximately, 2×10^6 cells containing 20% Matrigel (BD Biosciences,

Franklin Lakes, NJ) were injected into the mammary fat pat of female Balb/c nude mice. After the tumor volume reached 60 mm^3, the mice used for subsequent experiments.

Pharmacokinetic studies. Female six week old mice were used to study the pharmacokinetics. ^{DA}TAT-NP$_{IR\&DOX}$, ^{SA}TAT-NP$_{IR\&DOX}$, TAT-NP$_{IR\&DOX}$, and free DOX in PBS (0.01 M, pH 7.4) were injected intravenously into the tail vein with an equivalent DOX dose of 10 mg per kg of mouse body weight (n = 4 for each group). At a predetermined time, blood samples were collected from the retro-orbital plexus of the mouse eye, and 100 μL of plasma was obtained. After adding heparin, the plasma was extracted with chloroform/acetonitrile component solvent (1.0 mL, 4:1, v/v) on a vortex mixed for 1 min. Following centrifugation at a speed of 10000 g for 10 min, the organic phase was gathered and dried under vacuum condition, and added 100 μL DMSO to dissolve. The concentration of DOX was measured by UPLC. Pharmacokinetic parameters were calculated by non-compartmental data analysis of blood concentrations.

DOX distribution in major organs and tumor tissue. Mice bearing MDA-MB-231 tumors were treated with ^{DA}TAT-NP$_{IR\&DOX}$, ^{SA}TAT-NP$_{IR\&DOX}$, and TAT-NP$_{IR\&DOX}$ as described above. After 24 h, the mice were sacrificed, the solid tumor tissues were harvested, and the DOX accumulation in tumor tissue were detected by Xenogen IVIS® Lumina system and UPLC, respectively.

Temperature measurements during laser irradiation. Mice bearing MDA-MB-231 tumors were intravenous injected with 100 μL of ^{DA}TAT-NP$_{IR\&DOX}$, TAT-NP$_{IR\&DOX}$, ^{SA}TAT-NP$_{IR\&DOX}$, ^{DA}TAT-NP$_{IR}$/^{DA}TAT-NP$_{DOX}$, and IR&DOX (0.80 mg/mL of IR-780 and 0.4 mg/mL of DOX**)**. After 24 h post-administration, the tumors were irradiated by 808 nm

laser at power density at 1.0 W/cm^2 for 10 min. the real-time temperatures and infrared images were recorded using an infrared camera (ICI7320, Infrared Camera Inc., Beaumont, Texas, USA) and analyzed using IR Flash thermal imaging analysis software (Infrared Cameras Inc.)

***In vivo* tumor growth inhibition.** The Balb/c nude mice bearing MDA-MB-231 xenograft tumors were randomly divided into eight groups and were intravenously injected once every other days with 100 μL of PBS, free IR&DOX, TAT-NP$_{IR\&DOX}$, ^{DA}TAT-NP$_{IR\&DOX}$, and ^{SA}TAT-NP$_{IR\&DOX}$ (0.80 mg/mL of IR-780 and 0.4 mg/mL of DOX**)**. After 24 h of post-injection, the tumor tissue was locally irradiated by 808 nm NIR laser at a power of 1.0 W/cm^2 for 10 min. All of the treatments were repeated twice a week. The tumor volumes and changes in body weight of each mouse were monitored and recorded regularly, and the estimated volume was calculated according to the formula: tumor volume (mm^3) = 0.5 × length × width^2, following three weeks treatment, the tumor tissues of killed mice were excised to measure the weight.

Immunohistochemical analysis. One day after the last injection, the mice were sacrificed and tumor tissues were excised, fixed in 4% formaldehyde, and embedded in paraffin for analysis. Paraffin-embedded 5 μm tumor sections were obtained. Cell proliferation and apoptosis in tumor tissue were also analyzed by immunnohistochemical staining of the terminal transferase dUTP nick-end labeling (TUNEL) assay.

Statistical analysis. To measure significant differences among the treatment groups, statistical analyses were performed using Student's t-test. *$p < 0.05$ were considered to be

statistically significant, **p < 0.01 and ***p < 0.005 were considered to be highly significant.

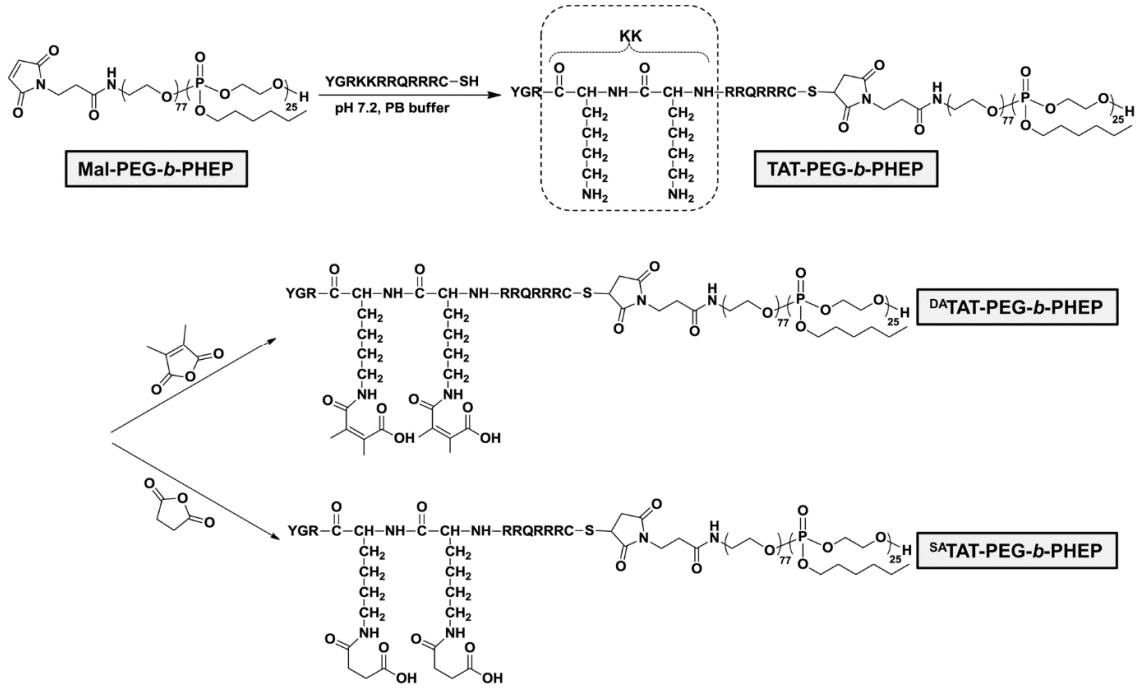

Scheme S1. Schematic illustration for the synthesis of TAT-PEG-*b*-PHEP and its derivatives.

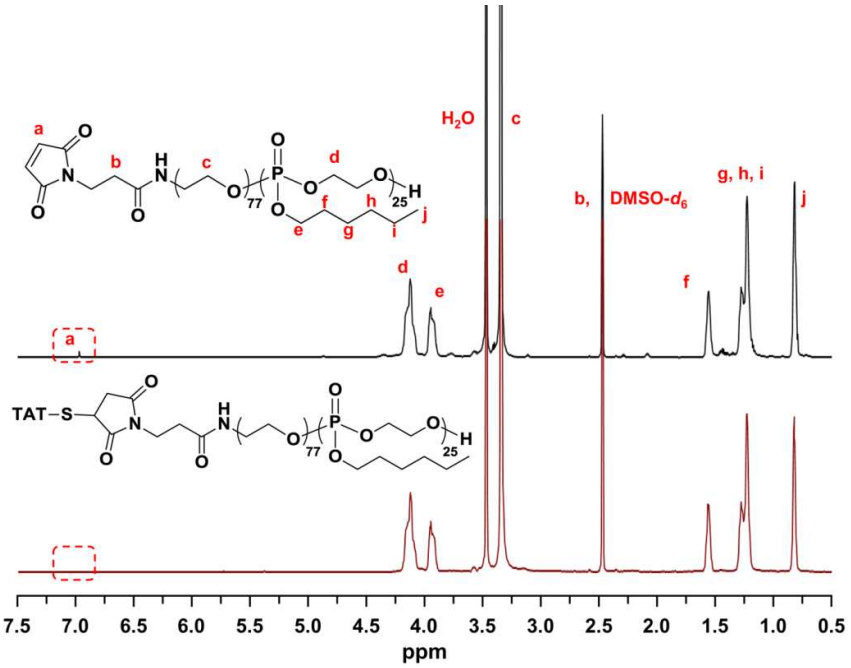

Figure S1. ^{1}H NMR spectra of Mal-PEG-*b*-PHEP and TAT-PEG-*b*-PHEP.

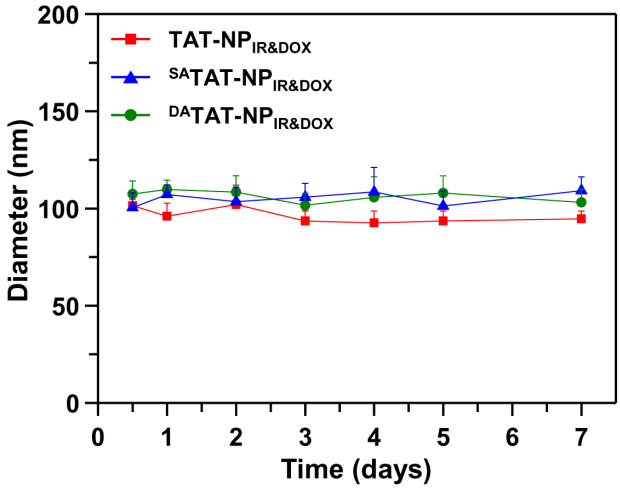

Figure S2. Changes in size of ^{DA}TAT-$NP_{IR\&DOX}$, ^{SA}TAT-$NP_{IR\&DOX}$, and TAT-$NP_{IR\&DOX}$ after incubation with culture medium containing 10% FBS.

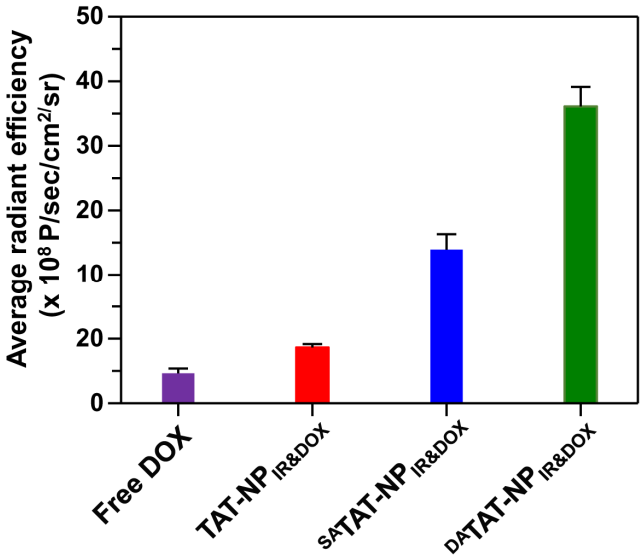

Figure S3. Quantification of DOX fluorescence in the tumors as performed in Figure 3A by the average radiant efficiency.

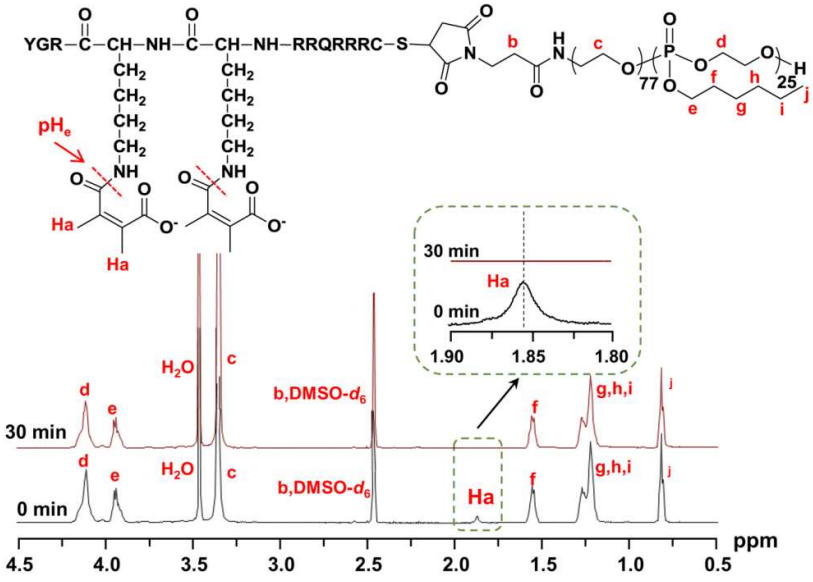

Figure S4. (A) ^{1}H NMR spectra of the blank nanoparticles ^{DA}TAT-NP after incubation at pH 6.5 for 30 min.

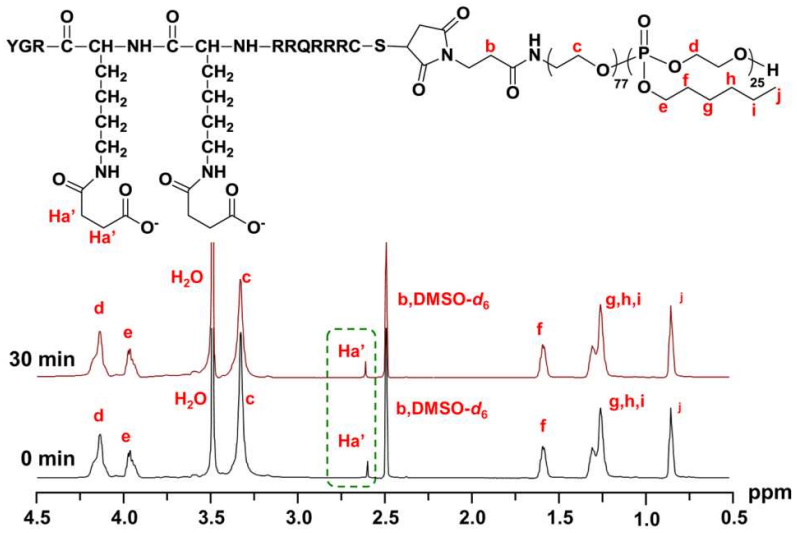

Figure S5. (A) ^{1}H NMR spectra of the blank nanoparticles ^{SA}TAT-NP after incubation at pH 6.5 for 30 min.

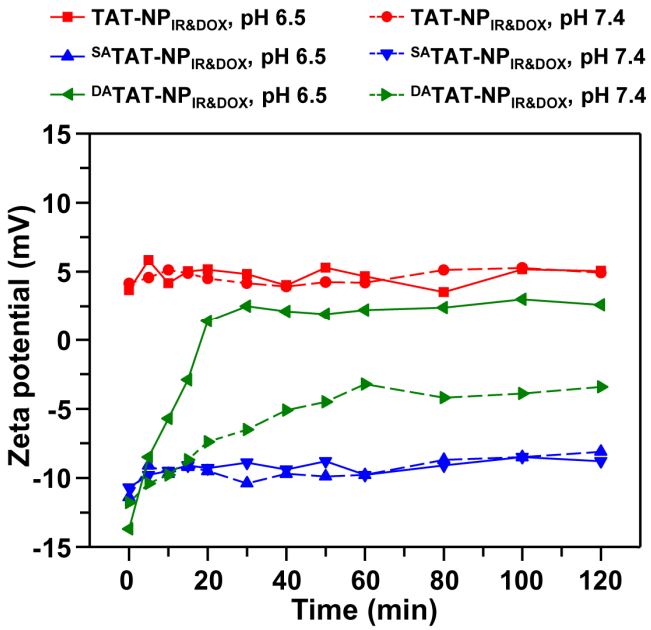

Figure S6. Zeta potential change of ^{DA}TAT-NP$_{IR\&DOX}$, ^{SA}TAT-NP$_{IR\&DOX}$, and TAT-NP$_{IR\&DOX}$ at pH 7.4 or 6.5.

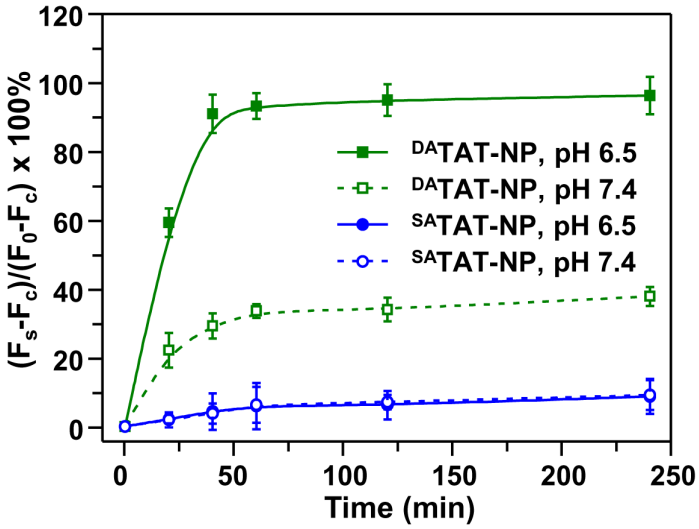

Figure S7. The degradation of ^{DA}TAT-NP and of ^{SA}TAT-NP at pH 7.4 and pH 6.5. Fluorescamine was used as the sensor.

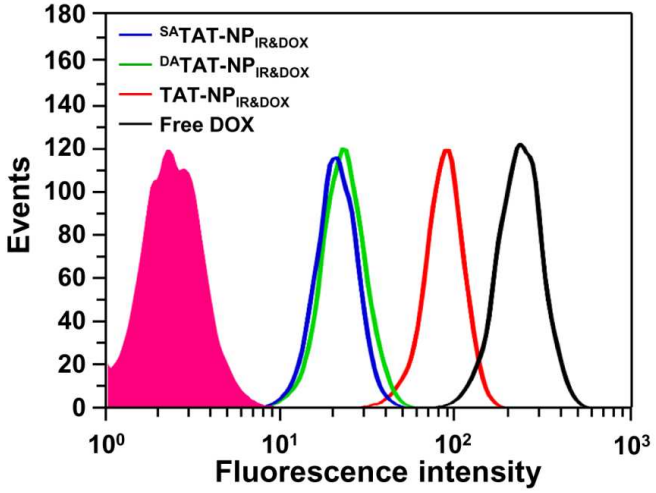

Figure S8. Flow cytometric analyses of MDA-MB-231 cells after incubation with ^{DA}TAT-NP$_{IR\&DOX}$, ^{SA}TAT-NP$_{IR\&DOX}$, and TAT-NP$_{IR\&DOX}$ at pH 7.4.

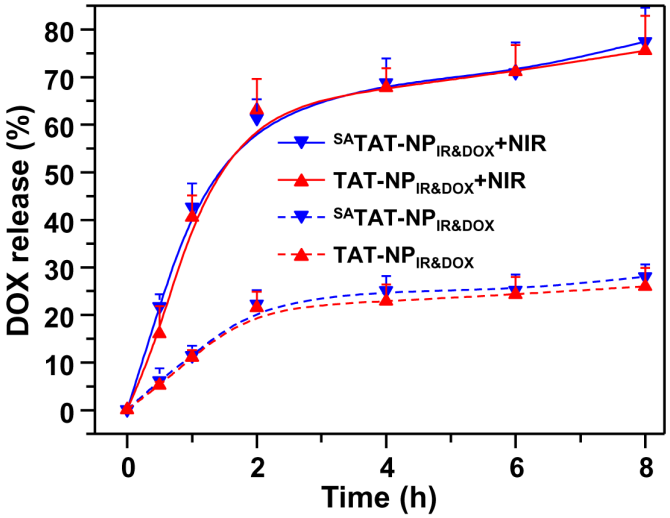

Figure S9. DOX release from ^{SA}TAT-NP$_{IR\&DOX}$ and TAT-NP$_{IR\&DOX}$ with or without NIR irradiation (808 nm, 1.0 W/cm^2, 5 min).

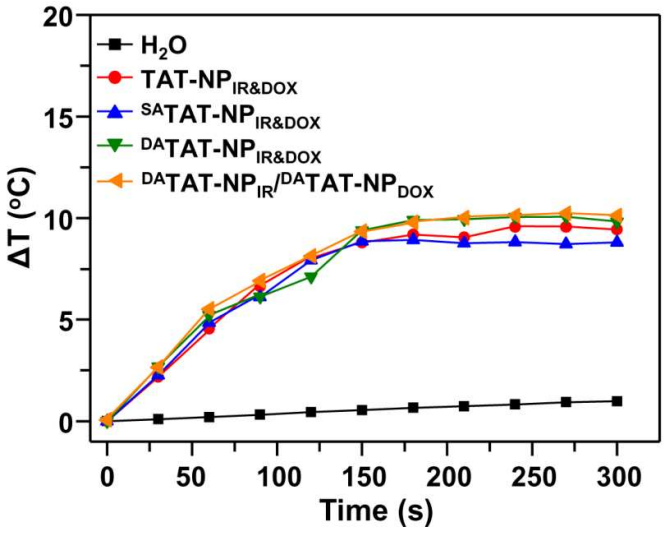

Figure S10. Temperature change curves of ^{DA}TAT-NP$_{IR\&DOX}$, ^{DA}TAT-NP$_{IR}$/^{DA}TAT-NP$_{DOX}$, ^{SA}TAT-NP$_{IR\&DOX}$, and TAT-NP$_{IR\&DOX}$ ([IR-780] = 2.0 μg/mL, [DOX] = 4.0 μg/mL) upon exposure to NIR laser (808 nm, 1.0 W/cm^2, 5.0 min).

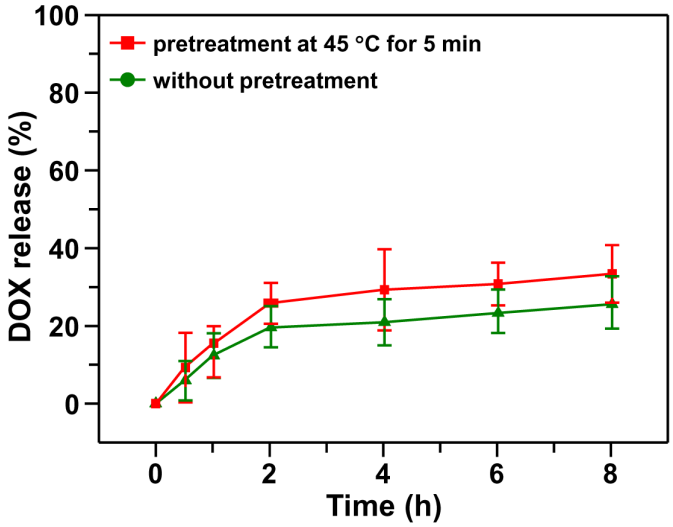

Figure S11. DOX release from ^{DA}TAT-NP$_{IR}$/^{DA}TAT-NP$_{DOX}$ after incubation in 37 °C or 45 °C water bath for 5 min.

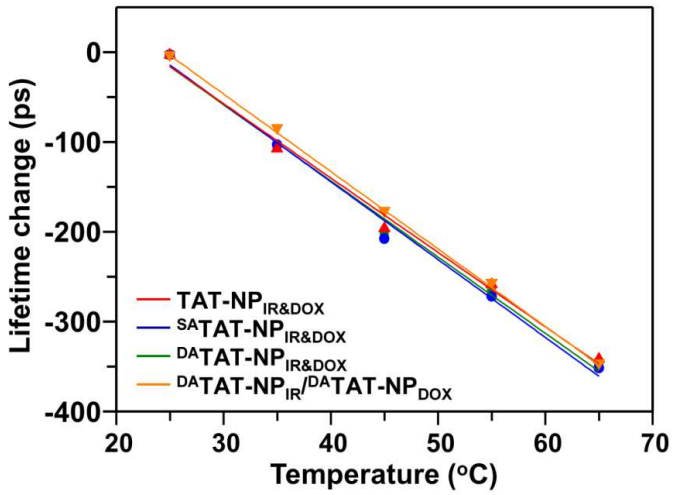

Figure S12. Change in average DOX lifetime (ps) of these formulations ([IR-780] = 2.0 μg/mL, [DOX] = 4.0 μg/mL) at various temperatures.

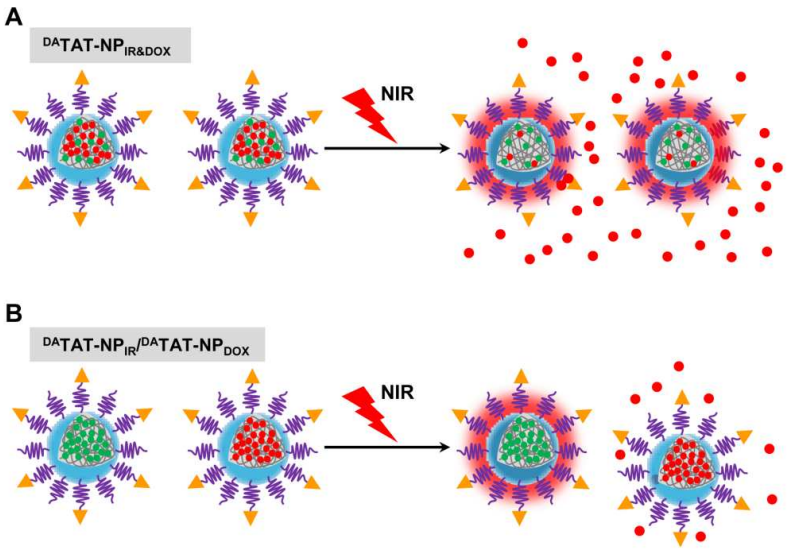

Figure S13. Schematic illustration of the different DOX release rate from ^{DA}TAT-NP$_{IR\&DOX}$ and ^{DA}TAT-NP$_{IR}$/^{DA}TAT-NP$_{DOX}$ under NIR irradiation.

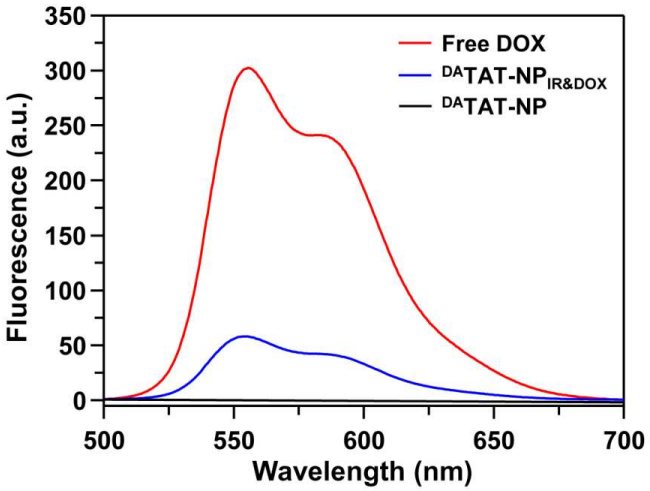

Figure S14. Fluorescent intensity of free DOX and ^{DA}TAT-NP$_{IR\&DOX}$ at the equivalent DOX concentrations (5.0 μg/mL).

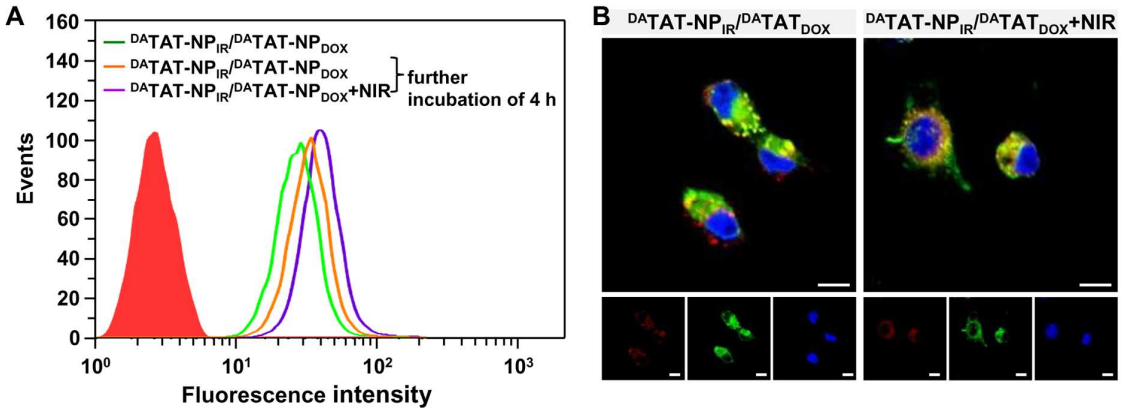

Figure S15. (A, B) Flow cytometric analyses (A) and CLSM images (B) of MDA-MB-231 cells after NIR irradiation (808 nm, 1.0 W/cm^2, 5 min) and further incubation 4 h. The MDA-MB-231 cells were pre-cultures with ^{DA}TAT-NP$_{IR}$/^{DA}TAT-NP$_{DOX}$ for 1 h. The scale bar is 10 μm.

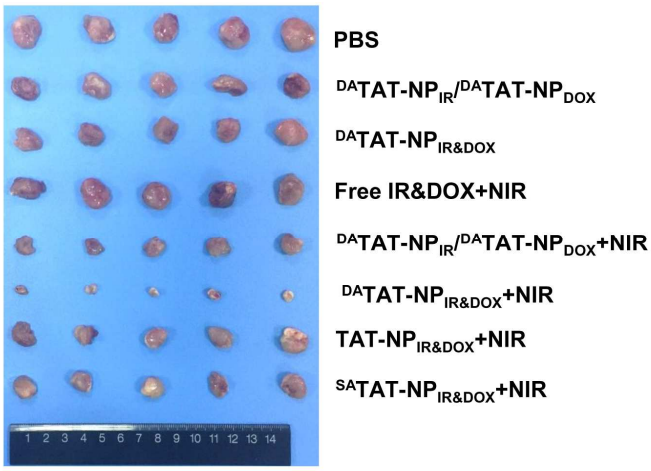

Figure S16. Tumor images of mice at the end time point of the treatment.

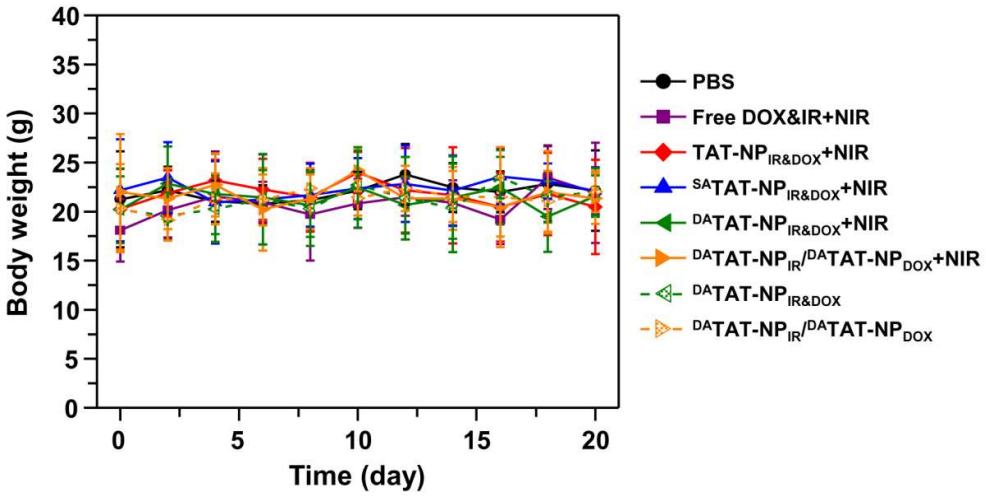

Figure S17. Body weight of mice bearing MDA-MB-231 tumor at different time points after treatment.

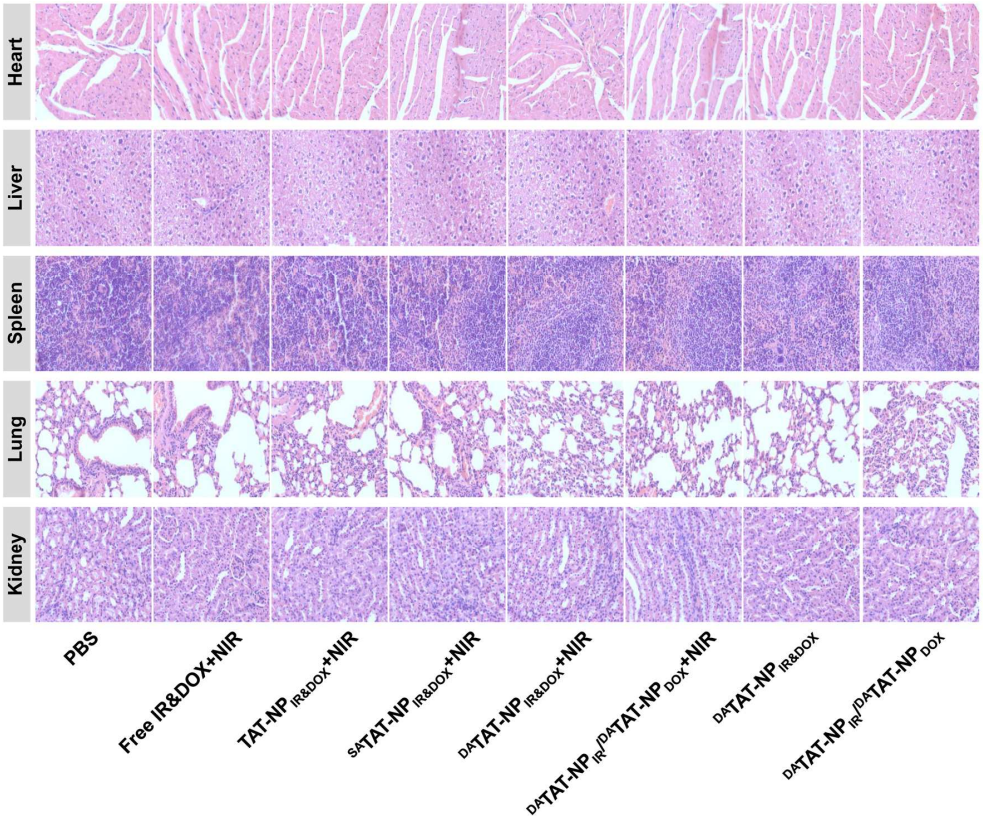

Figure S18. The H&E analysis of main organs after treatment with different formulation.

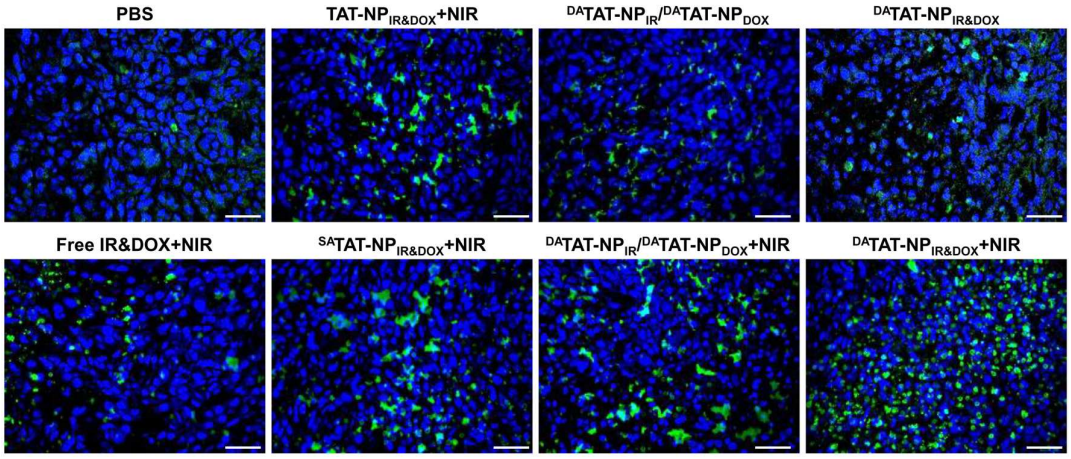

Figure S19. TUNEL analyses of tumor tissues after treatment**.** The scale bar is 10 μm.

Table S1. Pharmacokinetic parameters of these formulations after intravenous administration (n = 3 per group).

Parameter	C_{max} (μg/L)	T_{max} (h)	$AUC_{0\text{-}48h}$ (μg/L∗h)	Cl (L/h)
Free DOX	11.3	0.083	23.23	193.9
TAT-NP$_{IR\&DOX}$	28.3	0.083	33.75	64.5
^{DA}TAT-NP$_{IR\&DOX}$	65.9	0.083	124.69	14.2
^{SA}TAT-NP$_{IR\&DOX}$	63.0	0.083	134.03	13.0

C_{max}, Peak concentration;
T_{max}, Time at maximum concentration;
AUC, Area under curve;
Cl, Clearance rate;

REFERENCES

(1) Han, K.; Zhang, W. Y.; Zhang, J.; Lei, Q.; Wang, S. B.; Liu, J. W.; Zhang, X. Z.; Han, H. Y. *Adv.Func. Mater.* **2016,** *26*, 4351–4361.